Report for the Kavli Summer program in astrophysics held at the Max Planck Institute for Astrophysics during the summer of 2023

Constraining the results of nuclear fusion and mixing in the deep interiors of evolved massive stars using observations of stars stripped in binaries

F.D. Moyano[1], Y. Götberg, I. Caiazzo, and C. Wang

[1]University of Geneva, Switzerland
e-mail: facundo.moyano@unige.ch

September 21, 2023

ABSTRACT

Context. The interior of massive stars is not accessible in standard main sequence stars due to their thick hydrogen envelope. Therefore our understanding of stellar interiors in massive stars relies on observable properties at their surface. Stars that lost their hydrogen-rich envelope via binary interaction or stellar winds are useful objects to explore the interior of evolved massive stars simply from their surface properties.
Aims. By analysing and modelling the spectra of intermediate-mass stripped stars we aim at measuring the surface abundances of carbon, nitrogen, and oxygen (CNO).
Methods. We analyse the spectra of ten stars previously identified as stripped stars in binary systems where the stripped star dominates the flux in the optical to identify CNO lines. We then model their spectra with the non-LTE radiative transfer code CMFGEN with particular emphasis in reproducing the identified CNO lines.
Results. We identified several lines of highly ionised CNO elements in the sample of stripped stars and modelled the spectra of one of the stars, by exploring a range of different effective temperatures, and CNO abundances. We found that this star has a nitrogen abundance in rough agreement with the equilibrium abundance of the CNO cycle but shows a carbon abundance too high to be explained in absence of efficient mixing processes in deep radiative interiors.
Conclusions. The spectral characterisation of stars that lost a large part of their envelope can bring precise constraints on the physical processes operating in the stellar interior of massive stars.

Key words. stars: binaries – stars: interiors

1. Introduction

Massive stars are scarce and poorly understood in comparison to their lower-mass counterparts. Several uncertainties remain in our understanding of their stellar interiors, such as mixing processes induced by rotation or convective boundary mixing. They also develop strong stellar winds that could dominate their evolution at very late stages, or if their initial masses are high. Most of the massive stars observed to date were found in binary systems, indicating that the binarity fraction is relatively high in massive star compared to low-mass stars (Sana et al. 2012). Moreover, due to the short orbital period of the binary systems in which massive stars are found, a large fraction of them are expected to interact through their lives (de Mink et al. 2014), leading to interactions such as mass-transfer between the stars, or common-envelope evolution, or merger of the stars, among others.

In some cases, the mass-transfer can remove a large part of the hydrogen-rich envelope normally present in standard main sequence stars, thus revealing the inner stellar regions. If the mass-transfer occurs once the donor finished the core-hydrogen burning phase, then the removal of the envelope can reveal the products of the hydrogen nuclear burning phase. In massive stars, due to their high temperatures, the carbon-nitrogen-oxygen (CNO) (bi)cycle dominates the nuclear burning of hydrogen into helium which take place in the convective core that progressively becomes less massive during the main sequence. The CNO elements are catalysts of the reactions and during the cycle carbon- and oxygen-isotopes are transformed into nitrogen. Thus probing the surface abundance of stripped stars would give direct information on the interior of main sequence stars.

Stripped stars are expected to be seen as helium enriched stars, with little to no hydrogen at their surface, and high surface gravities and effective temperatures (e.g. Götberg et al. 2017) ; stars with those properties are known as hot subdwarfs in the low-mass range and Wolf-Rayet stars in the high-mass range. However they can also have high abundance of heavier elements such as carbon in WC stars (e.g. Grafener et al. 1998) or in hot subdwarfs (e.g. Heber 2016). Until recently, a firm detection of the intermediate-mass component remained elusive, but a few tens of objects were observed to have properties in agreement with estimations of binary stellar evolution models (Ramachandran et al. 2023; Drout et al. 2023).

In this work we reanalyse the subsample of stars studied by Drout et al. (2023), focusing on the stars in which the stripped star dominate the optical flux of the binary (or multiple) system. Gotberg et al. (2023) constrained the main properties of these ten stripped stars, determining so their effective temperatures, luminosities, surface gravities, and surface abundance of hydrogen and helium. Our aim is to complement these properties by deriving the surface-abundance of heavy elements expected from the core-hydrogen burning phase, namely carbon, nitrogen, and oxygen.

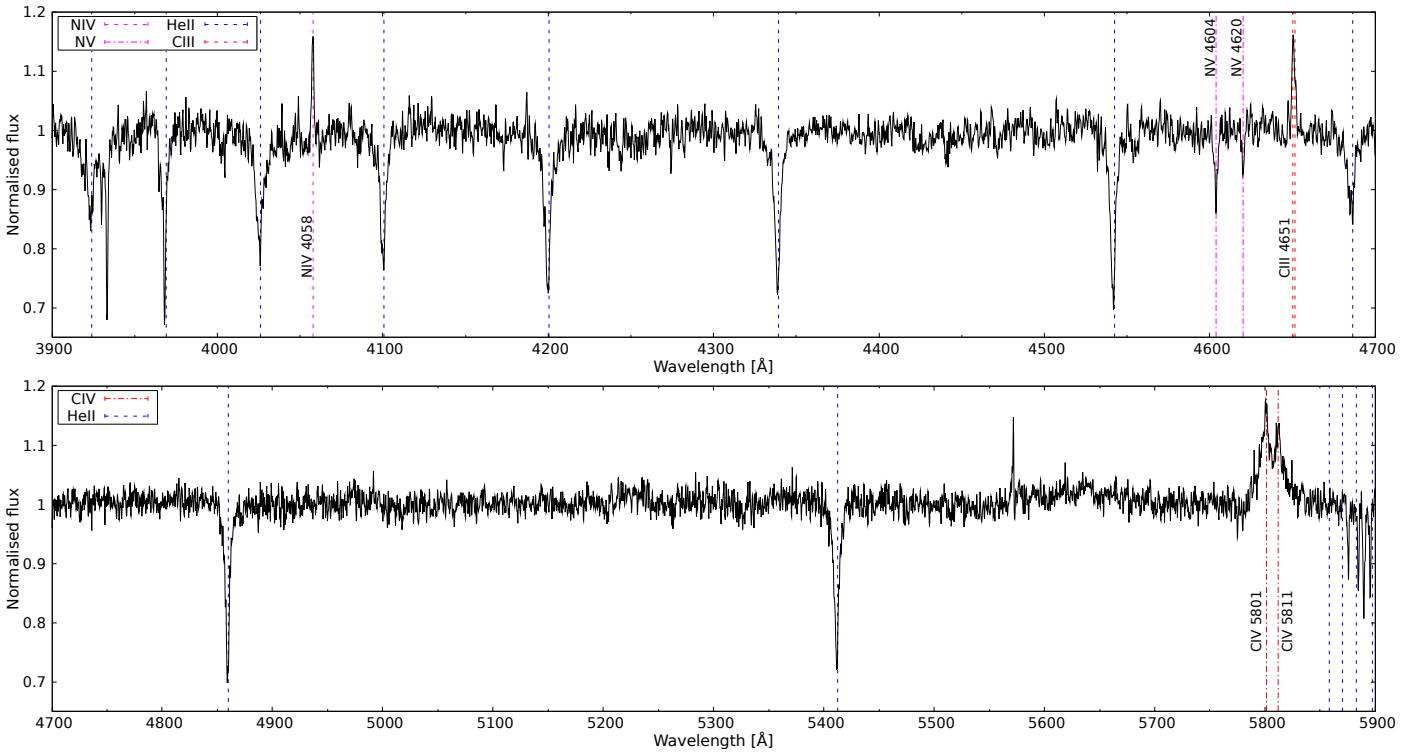

Fig. 1. Normalised spectrum of the star analysed. The upper panel shows the blue part of the spectrum covering the wavelength range from 3900 to 4700 Å while the lower panel shows the red part covering the wavelength range from 4700 to 5900 Å. The location of the ionised helium lines are indicated in blue and the lines of nitrogen and carbon identified in the spectrum are labelled with their corresponding wavelengths.

2. Methods

We start our study from the normalised spectra presented by Gotberg et al. (2023), which were obtained using the *The Magellan Echellette (MagE)* spectrograph on the Magellan/Baade 6.5m telescope. The spectra have medium resolution (R $\simeq$ 4100) and cover the optical range ($\lambda \simeq 3700 - 7000$Å) [1]. Using the normalised spectra of the ten stars where the stripped star dominates the optical flux, we identified the CNO lines in the spectrum of the stars by comparing the wavelength at which the lines of ionised CNO elements are expected to form, according to the NIST database [2]. In this work we present the analysis of the CNO lines of one of the stars, whose spectrum is shown in Fig. 1; the rest of the sample also contains several lines of ionised CNO elements which will be the topic of a follow-up work.

We analyse in detail one of the stars, which has the lowest surface hydrogen abundance of the sample, and thus shows a high abundance of helium. This star has an effective temperature of $T_{\rm eff} = 66^{+18}_{-7}$kK, a surface gravity of $\log g = 4.5 \pm 0.3$, a bolometric luminosity of $\log(L/L_\odot) = 4.3^{+0.3}_{-0.2}$, and surface abundances of hydrogen and helium of $X_{\rm H} = 0.01^{+0.04}_{-0.00}$ and $X_{\rm He} = 0.98^{+0.00}_{-0.04}$, respectively (Gotberg et al. 2023). We identified the following lines of ionised CNO elements in this star: CIII λ4651, CIV λ5801/11, NIV λ4058, NV $\lambda\lambda$4604,20, shown in Fig. 1. Those lines are isolated from strong He lines and so can be used as reliable indicators of surface abundances of CNO.

To estimate the surface abundances of CNO elements we used the non-LTE radiative transfer code CMFGEN (Hillier 1990; Hillier & Miller 1998) to compute the model atmospheres and synthetic theoretical spectra. We computed atmosphere models starting from the parameters corresponding to the best-fit models previously mentioned and presented by Gotberg et al. (2023), which can reproduce the helium spectral lines. However the effective temperature is not very well constrained by helium lines, but nitrogen and carbon lines are much more sensitive to temperature variations because of their larger number of electrons, thus we also vary the effective temperature in our analysis. Then to study how the sensitivity of the CNO features change with the atmosphere parameters we computed models with effective temperatures in the range $T_{\rm eff} = 54000 - 72000K$, and different surface nitrogen abundances in the range $X_{\rm N} = 10^{-3} - 4 \times 10^{-3}$, and surface carbon abundances in the range $X_{\rm C} = 4 \times 10^{-5} - 10^{-3}$, keeping the abundance of helium and the sum of CNO elements constant, which leads to oxygen abundances in the range $X_{\rm O} = 10^{-4} - 3 \times 10^{-3}$. The effect of these parameters on the profile of the nitrogen lines is shown in Fig. 2.

We then compute the equivalent width (EW) of the lines for each model and compare them to the EW of the lines in the observed spectrum. The equivalent width (EW) is computed as

$$\mathrm{EW} = \int_{\lambda_1}^{\lambda_2} 1 - \frac{f_\star}{f_{\rm c}} d\lambda \qquad (1)$$

where λ_1, λ_2 are the lower and upper limits of the wavelength for a given line, $f_\star$ is the flux of the star taking into account the absorption or emission of the spectral line, and $f_{\rm c}$ is the continuum-flux. For absorption lines the EW is positive while for emission lines it is negative; if no line is present then the EW is zero. Then the measured EW of the lines is compared to the one obtained from the atmosphere models. We use this method to constrain the surface abundance of CNO elements, since the EW is conserved irrespective of the shape of the line and thus to other effects on

[1] See Drout et al. (2023) for more details
[2] https://www.nist.gov/pml/atomic-spectra-database

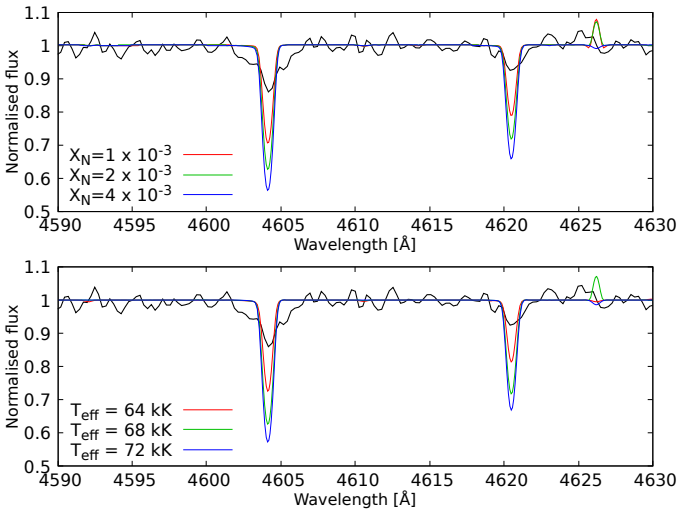

Fig. 2. Observed spectrum (black) and synthetic spectra around the region of NV 4604 and NV 4620 lines. The top panel shows the effect of the abundance of nitrogen while the bottom panel shows the effect of the temperature adopted in the models.

the lines such as rotational broadening, macroturbulence, among others.

3. Results

To constrain the abundance of nitrogen, we use the three lines of ionized nitrogen identified in the spectrum, namely: NIV λ4058, NV λ4604, and NV λ4620. The comparison of the EW of each line for different temperatures and abundances of nitrogen is shown in Fig. 3. The EW of the NIV λ4604 and NIV λ4620 lines increases with temperature because the line is highly sensitive to temperature, as shown in Fig. 2. We also show the dependence on nitrogen abundance; the lines have a similar degree of sensitivity to the assumed nitrogen abundance or temperature. Similar trends are found for the NIV λ4058 line, which is an emission line in this star rather than an absorption line, and thus its EW is negative, formed mainly by 'two-electron' transitions (Rivero González et al. 2012). From the comparison of the EW between models and the observed spectrum, we can give an initial estimate of $X_{\rm N} = (2 \pm 1) \times 10^{-3}$. We did not use the CIII λ4651 line as it is challenging to model and uncertainties on atomic data and could to wrong estimations of at least a factor two (Martins & Hillier 2012); on the other hand the CIV $\lambda\lambda$5801/11 lines are reliable indicators of carbon abundance (Carneiro et al. 2018). The carbon lines CIV $\lambda\lambda$5801/11 are very close to each other (see Fig. 1) and so we decided to treat them as a single line by measuring the EW of both lines together. We computed models with various abundances of carbon in the range $X_{\rm C} = 10^{-5} - 10^{-3}$ and different temperatures, but none of the models can match the EW of the observed line. The comparison of the equivalent widths for this doublet is shown in Fig. 4. This indicates that the abundance of carbon at the surface is high; we give an initial lower boundary for its abundance of $X_{\rm C} > 10^{-3}$.

4. Discussion and conclusions

The estimated abundance of nitrogen is in the range expected for equilibrium abundances of the CNO cycle, where it is expected that $\simeq$ 98% of the initial abundance of carbon, nitrogen, and oxygen is transformed into nitrogen. From binary stellar evolution models, we expect stars that lost a large part of their envelope to have abundances of nitrogen around $X_{\rm N} \simeq 10^{-3}$. This is because in our stellar evolution models the surface abundances

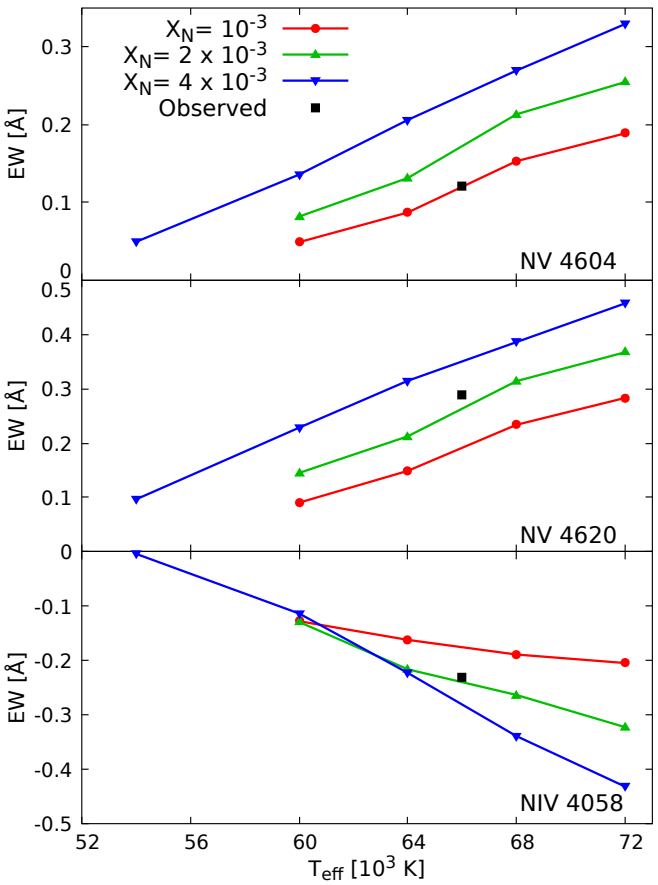

Fig. 3. Equivalent width of the nitrogen lines of the synthetic spectra and the observed spectrum as a function of the effective temperature. The models were computed with different abundances of nitrogen as indicated in the legend of the top panel; each panel corresponds to one line as indicated in the legend on the corner.

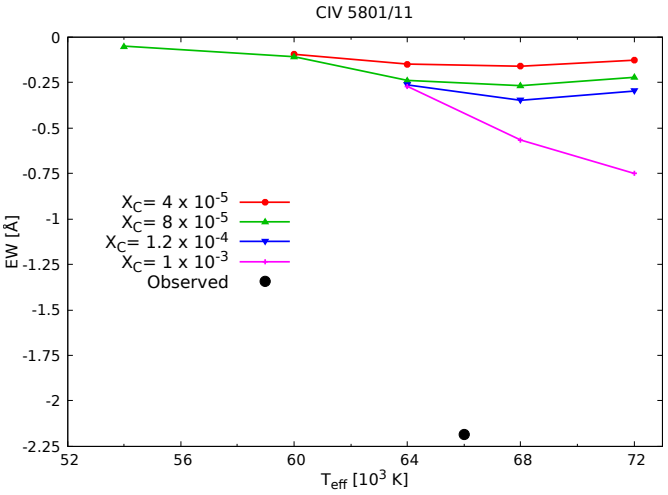

Fig. 4. Equivalent width of the doublet CIV 5801/11 line of the synthetic spectra and the observed spectrum as a function of the effective temperature. The models were computed with different abundances of carbon as indicated in the legend.

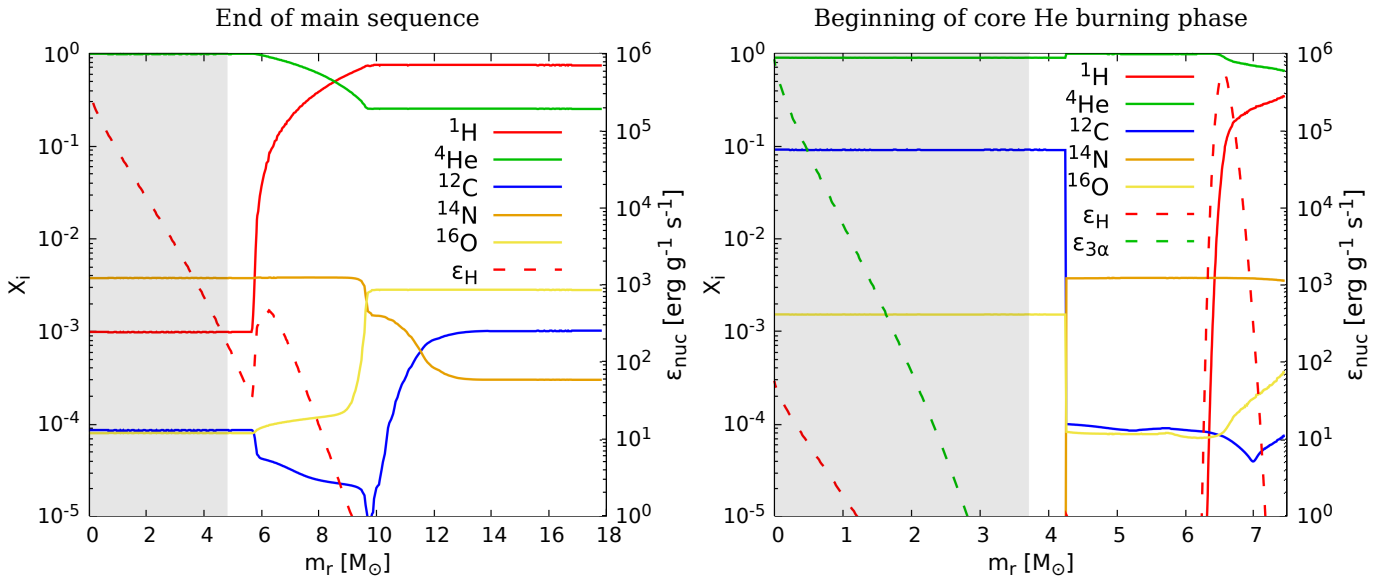

Fig. 5. Profile of chemical abundances in mass fraction and nuclear energy generation rate near the end of the main sequence (left) when the central hydrogen abundance is $X_{\rm H} = 10^{-3}$ and at the beginning of the core-helium burning phase when $X_{\rm He} = 0.9$.

reflect the equilibrium abundances resulting from the hydrogen burning phase at the very early stages of the main sequence, when the convective core had its largest extent; then the convective core retreats until it vanishes at the end of the main sequence. This is shown in Fig. 5, where we show the profiles of the chemical abundances through the whole star near the end of the main sequence, and at the beginning of the core-helium burning phase, for a model of the donor with an initial mass 18.17 $M_\odot$. At the beginning of the core-helium burning phase, the star already lost $\sim 11 M_\odot$, and so the abundance of nitrogen is the equilibrium abundance of the CNO cycle, i.e. when most of the carbon and oxygen is transformed into nitrogen. For the metallicity adopted in these models, which corresponds to the metallicity of the LMC and thus to a value of $Z = 0.006$, the nitrogen abundance resulting from the CNO cycle and thus the surface abundance during the stripped phase is $X_{\rm N} \simeq 4 \times 10^{-3}$, and its value is roughly independent of the initial stellar mass of the donor. This value is in good agreement with the estimated value of $X_{\rm N} = 2 \pm 1 \times 10^{-3}$ from the spectrum.

However, the abundance of carbon in our models is $X_{\rm C} \simeq 4.5 \times 10^{-5}$ at the middle of core-helium burning phase. This value is lower by at least two orders of magnitude than that estimated in the star, which is at least $X_{\rm C} = 10^{-3}$ based on the comparison between the EW of the atmosphere models and the spectrum of the CIV 5801/11 doublet. To have such a high abundance of carbon at the surface, the star should have lost enough mass to expose its carbon-core (or the regions near to it), as in the case of Wolf-Rayet carbon-stars (WC type;e.g. Koesterke & Hamann 1995; Grafener et al. 1998). However this seems unlikely since the lower luminosities and spectroscopic mass inferred for this star would point out to a less massive convective core during the stripped phase. Another possibility is that the carbon resulting from the core-helium burning phase is transported to the surface of the star by some mechanism operating in radiative regions, such as rotational mixing or internal gravity waves. This star could represent the hotter counterpart of carbon-rich He-sdO stars (e.g. Heber 2016) and the cooler counterpart of WC stars. A more detailed analysis and an extension of this study to other stripped stars is necessary to confirm whether this is a common feature in intermediate-mass stripped stars.

Acknowledgements. FDM received funding from the European Research Council (ERC) under the European Union's Horizon 2020 research and innovation programme (grant agreement No. 833925, project STAREX).

References

Carneiro, L. P., Puls, J., & Hoffmann, T. L. 2018, A&A, 615, A4
de Mink, S. E., Sana, H., Langer, N., Izzard, R. G., & Schneider, F. R. N. 2014, ApJ, 782, 7
Drout, M. R., Götberg, Y., Ludwig, B. A., et al. 2023, arXiv e-prints, arXiv:2307.00061
Götberg, Y., de Mink, S. E., & Groh, J. H. 2017, A&A, 608, A11
Gotberg, Y., Drout, M. R., Ji, A. P., et al. 2023, arXiv e-prints, arXiv:2307.00074
Grafener, G., Hamann, W. R., Hillier, D. J., & Koesterke, L. 1998, A&A, 329, 190
Heber, U. 2016, PASP, 128, 082001
Hillier, D. J. 1990, A&A, 231, 116
Hillier, D. J. & Miller, D. L. 1998, ApJ, 496, 407
Koesterke, L. & Hamann, W. R. 1995, A&A, 299, 503
Martins, F. & Hillier, D. J. 2012, A&A, 545, A95
Ramachandran, V., Klencki, J., Sander, A. A. C., et al. 2023, A&A, 674, L12
Rivero González, J. G., Puls, J., Najarro, F., & Brott, I. 2012, A&A, 537, A79
Sana, H., de Mink, S. E., de Koter, A., et al. 2012, Science, 337, 444